Geomechanics and Engineering, *Vol. 35, No. 6 (2023) 581-591*
https://doi.org/10.12989/gae.2023.35.6.581

Earthquake hazard and risk assessment of a typical Natural Gas Combined Cycle Power Plant (NGCCPP) control building

A. Can Zülfikar*[1], Seyhan Okuyan Akcan[2a], Ali Yeşilyurt[1], Murat Eröz[3] and Tolga Cimili[3]

[1]*Istanbul Technical University,Disaster Management Institute ,Istanbul,34469,Turkey*
[2]*Boğaziçi University,Civil Engineering Department,Istanbul,34342,Turkey*
[3]*Asset Management and Sustainability , EnerjiSA Üretim, Istanbul, 34746, Turkey*

(*Received November 12, 2022, Revised October 15, 2023, Accepted November 23, 2023*)

Abstract. North Anatolian Fault Zone is tectonically active with recent earthquakes (Mw7.6 1999-Kocaeli and Mw7.2 1999-Düzce earthquakes) and it passes through Marmara region, which is highly industrialized, densely populated and economically important part of Turkey. Many power plants, located in Marmara region, are exposed to high seismic hazard. In this study, open source OpenQuake software has been used for the probabilistic earthquake hazard analysis of Marmara region and risk assessment for the specified energy facility. The SHARE project seismic zonation model has been used in the analysis with the regional sources, NGA GMPEs and site model logic trees. The earthquake hazard results have been compared with the former and existing earthquake resistant design regulations in Turkey, TSC 2007 and TBSCD 2018. In the scope of the study, the seismic hazard assessment for a typical natural gas combined cycle power plant located in Marmara region has been achieved. The seismic risk assessment has been accomplished for a typical control building located in the power plant using obtained seismic hazard results. The structural and non-structural fragility functions and a consequence model have been used in the seismic risk assessment. Based on the seismic hazard level with a 2% probability of exceedance in 50 years, considered for especially these type of critical structures, the ratios of structural and non-structural loss to the total building cost were obtained as 8.8% and 45.7%, respectively. The results of the study enable the practical seismic risk assessment of the critical facility located on different regions.

Keywords: earthquake risk analysis; economical loss; fragility functions and consequence models; natural gas combined cycle power plant; probabilistic earthquake hazard analysis

1. Introduction

In today's world, the demand for energy is increasing rapidly for all societies. In parallel to this, the need for electricity consumption also increases day by day. Almost all modern and critical infrastructure systems are dependent on electricity and "Electricity Generation and Distribution" become one of the most important and strategic elements. It is a fact that including Sustainability perspective, the continuity of "Electricity Generation and Distribution" in all conditions including disaster situations is a very important requirement.

Electricity networks are one of the critical infrastructures with high probability of damage due to earthquake hazards. These systems can be investigated within three main groups as generation facilities, transmission and distribution network. Damage to any sub-element of these three main classes may cause disruption of the entire system (Massie and Watson 2011). Failures in these systems will cause discontinuity of modern life, emergency services and the discontinuity of the functionality of various infrastructures. It has a direct impact on economic and social life, as it is one of the main needs for the continuity of commercial and industrial activities in the region where the electrical power system is located. During the field studies carried out after past earthquakes, it was observed that generation and distribution were disrupted due to local damages in the electricity networks and these malfunctions could continue in the relevant regions during the repair / maintenance period.

Severe damages occurred in two important electricity generation facilities during the Mw9.0 Tohoku earthquake, Japan on March 11, 2011. The 6-day renovation works were carried out in order to eliminate the aforementioned damages and restore electricity generation, the facility was put into operation around 90% (Eidinger *et al.* 2012). As a result of the earthquakes of 4 September 2010, Mw7.1 Darfield (Canterbury), 22 February 2011, Mw6.3 Christchurch and 13 June 2011, Mw6.0 Christchurch, New Zealand, the damages were observed in the electricity transmission and in the switchyard where the distribution is made. Light and medium damages were detected in 220 kV CVT, 66kV transformer porcelain bushings, porcelain support insulators, cutters, pantograph separators and equipment (mechanical-electrical accessories and contents) in the control building. When these three earthquakes are considered separately, these facilities have been reactivated in less than 6 hours immediately after the earthquakes

*Corresponding author, Associate Professor
E-mail: aczulfikar@itu.edu.tr
[a]Ph.D. Student

ISSN: 2005-307X (Print), 2092-6219 (Online)

Fig. 1 EnerjiSA Üretim Bandırma-I natural gas combined cycle power plant

(a) 8.4 magnitude Peru Earthquake, 2001; Suspended ceiling, lighting, insulation damages in the Industrial Plant Control Building

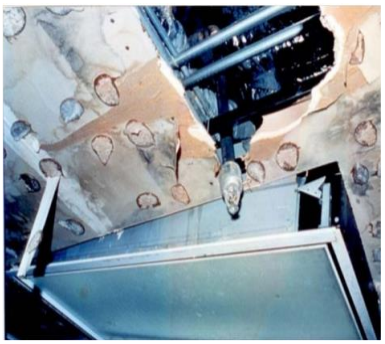

(b) 6.7 Magnitude Northridge Earthquake, 1994; Fire extinguishing system pipes and sprinkler system damages in Olive View Hospital

(c) 8.8 Magnitude Chile Earthquake, 2010; HVAC equipment damage in Santiago Airport Terminal Building

Fig. 2 Equipment damages of past earthquakes

(Giovinazzi *et al*. 2011, Transpower 2011a). As a result of the Mw7.2 Mexico earthquake on April 4, 2010, damages occurred in the support connections of the busbars, porcelain surge arrester, transformer porcelain bushings and normal separators located in the San Diego Gas and Electric (SDG & E) Substation. Determination of critical elements and alternative strengthening studies were investigated for the mentioned facility (Howard 2015). In the study of M. Shinozuka *et al*. (2005), a relationship was established between the risk curves and economic parameters by considering 47 earthquake scenarios for the Los Angeles Department of Water and Power's (LADWP's) electric power plant. Similarly, studies in the literature consider different methods and approach for seismic vulnerability assessment of electrical power plants (Park *et al*. 2006, Buritica Cortes *et al.* 2015, Kwasinski *et al.* 2014, Li *et al*. 2014, Yesilyurt *et al*. 2021).

When all past earthquakes are examined, it is seen that most earthquake damages were caused by non-structural elements and equipment (FEMA E -74, 2011). Some damaged photos were shown in Fig. 2. In general, the ratio of financial losses to the construction cost of the building due to non-structural elements and equipment damages has been found to be up to 65% -85% for typical commercial buildings, and in-hospital buildings, this rate can be 2 to 3 times higher (FEMA E -74,2011). Considering the high-cost equipment used in power plants, it can be predicted that the cost rates of equipment damage will be much higher. In addition, non-structural damages may cause losses in roduction in power plants due to the stoppage of the operation, and thus the commercial losses can be well above the potential structural and/or non-structural losses costs.

Non-structural elements and equipment in buildings are architectural, mechanical, electrical installations, and even furniture. All kinds of equipment, windows, partition walls, pipes, suspended ceilings, air ducts, elevators, computers/servers, filing cabinets are vulnerable to earthquake damage (Villar-Vega *et al.* 2017).

As it is shown in Fig. 3, EnerjiSA Üretim Bandırma-I Natural Gas Combined Cycle Power Plant (NG-CCPP) (Fig. 1) is located in Bandırma town of Balıkesir City, Marmara region in Turkey. The power plant with an installed capacity of 936 MW has two gas turbines each with a capacity of 304.29 MW, two heat recovery steam generators with a steam capacity of 500 tons/hour and a steam turbine with a capacity of 327.6 MW. The power plant is located close to the Marmara Sea and sea water is used for cooling purposes with the amount of 54.000 m3/hour. The connection of the power plant to the national electricity network is provided over the 380 kV switchyard over the "Bursa NG-CCPP" and "Karabiga" High Voltage lines, as detailed in Fig. 3b. In addition, a 3.45 MW hydroelectric power plant was commissioned to meet the internal needs of the natural gas power plant. The annual average power generation capacity of the plant is 7.9 TWh.

Earthquake risk assessment is a fundamental step for the creation and implementation of disaster risk reduction (DRR) measures (Villar-Vega *et al*. 2017, Mousapoor *et al*.

(a) Location (b) Residential

Fig. 3 EnerjiSA Üretim Bandırma-I Natural Gas Combined Cycle Power

2020). After determining the buildings that are at risk will be taking emergency measures in these buildings, if necessary to strengthen or demolish and minimize the loss of lives from a possible earthquake (Kepenek *et al.* 2020, Pourkeramat *et al*. 2021).

Earthquake risk models are developed using a probabilistic seismic hazard model, an exposure model that includes information on the elements exposed to the hazard (e.g. buildings, population) and a set of vulnerability functions that determine the probability of loss depending on the level of ground shaking. (Villar-Vega *et al*. 2017). In earthquake risk analysis, fragility functions that determine the probability of exceeding each damage state of structures are important. (Villar-Vega *et al*. 2017).

Within the scope of this study, the Seismic Hazard analysis for the " Bandırma-I Natural Gas Combined Cycle Power Plant", in which the production capacity and components are explained in detail, is carried out through OpenQuake, an open source program, considering the tectonic structure, seismicity and seismic source zoning of the area. The economic losses due to seismic hazard were calculated using the seismic risk operator of the OpenQuake-engine. Probabilistic seismic risk assessment in financial loss assessment of the control building, which is one of the most important structures in order to ensure the continuity of operation and production, was assessed by considering structural damage and damage to equipment (mechanical-electrical accessories and contents) through the "Fragility Curves". In the light of these assessments, probabilistic damage costs that may occur in the control building in various earthquake scenarios were calculated by using "Vulnerability Curves". The studies carried out have yielded significant results for the development of post-earthquake action plans, risk assessment and mitigation studies, and the reinsurance assessment of the power plant.

In this study, a rapid earthquake risk assessment of EnerjiSA Üretim Bandırma-I Natural Gas Combined Cycle Power Plant was performed by identifying critical elements that may cause power generation interruption. This method can be practically adapted for different energy facilities globally.

2. Method

2.1 Marmara region earthquake hazard analysis

Seismic risk assessment and loss estimation are the basic prerequisites for reducing the destructive effects caused by earthquakes (Martins *et al.* 2020).To perform the seismic risk analysis, it is necessary to use a reliable seismic hazard model, a comprehensive building inventory model and a set of fragility and vulnerability functions (Martins *et al*. 2020). As a result of the seismic risk assessment, the distribution of loss rates with the probability of exceeding are calculated. That is, the results of risk analysis are used to take measures to reduce potential losses from possible earthquakes (Silva *et al.* 2015).

The Global Earthquake Model (GEM) aims to calculate the earthquake risk worldwide (Silva *et al*. 2013b). For this purpose, an open source OpenQuake software for seismic hazard and risk assessment is developed by GEM. The OpenQuake project (http://www.globalquakemodel.org/openquake/) was launched as part of the Global Earthquake Model (GEM (http://www.globalquakemodel.org) (Pinho 2012)). OpenQuake is an open-source web-based seismic assessment platform written in Python programming language for modeling and analyzing earthquake hazards and the resulting risk of earthquakes (Silva *et al.* 2013b). The software consists of a set of calculators that can perform scenario-based or probabilistic seismic hazard analyses and calculate human or economic losses for a collection of assets (Burton and Silva 2016).

Hazard describes the probability of occurrence of unexpected events that may endanger the structure, such as natural disaster, while structural vulnerability refers to the susceptibility of the structure when subjected to hazard (Fujino *et al.* 2009). The seismic hazard assessment of a region requires knowledge about the tectonic structure of the region, earthquake occurrences, and local ground conditions. The probabilistic seismic hazard analysis model constitutes seismic data of the region the ground motion prediction equations that can be used in the region. With the OpenQuake program, seismic risk assessment is performed depending on the results obtained from deterministic or probabilistic earthquake hazard analysis.

Basic components of Probabilistic Seismic Hazard Assessment (PSHA); identification of earthquake source (s), earthquake occurrence characteristics of each defined source and ground motions prediction equations. This information is numerically integrated using a probabilistic

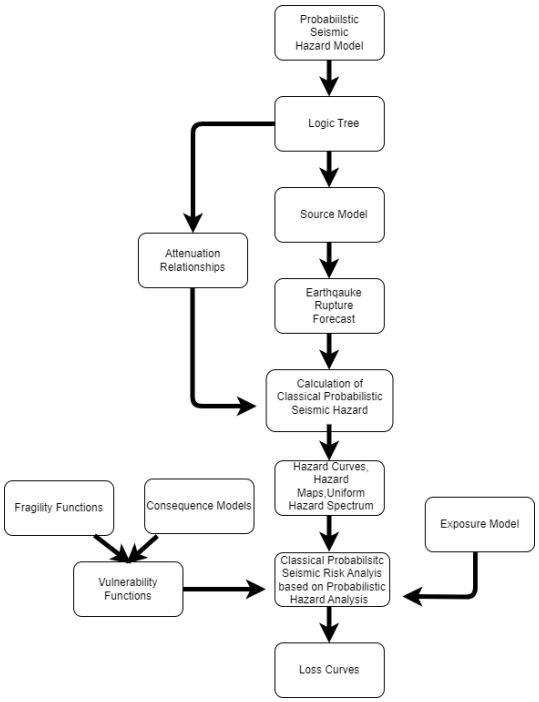

Fig. 4 Earthquake risk calculation flow chart based on classical probabilistic seismic hazard

model to obtain the probability of exceeding different ground motion intensity levels in each region (Cornell 1968). Probabilistic seismic hazard analysis enables the calculation of loss probability and loss statistics for a single asset, based on a probabilistic definition of the hazard (Silva *et al.* 2013b). The seismic risk is assessed by identifying and understanding the nature of hazard and vulnerability of structure (Fujino *et al.* 2009). As a result of the seismic hazard analysis, hazard curves, site-specific spectrum, and hazard maps are obtained, while the loss and damage distribution are calculated as a result of the seismic risk analysis. Fig. 4 shows the probabilistic seismic risk analysis flow chart by considering probabilistic seismic hazard analysis.

OpenQuake, the PSHA-based damage calculator, combines the seismic hazard curve at the location of the asset with the separate or continuous damage vulnerability functions for an asset through numerical integration to give the asset damage distribution over a specified period. It is assumed that the continuous fragility functions are well represented by the cumulative distribution function of the lognormal distribution for OpenQuake analysis steps (Pagani *et al.* 2014).

Probabilistic seismic risk assessment is used to calculate the possible loss that will occur in buildings as a result of possible earthquakes and to take necessary measures (Torbo 2015). Seismic fragility and loss model assessment is an important step in assessing the probabilistic seismic risk of a region (Martins *et al.* 2020). Fragility is defined as the probability of exceeding the damage limit state corresponding to a set of seismic intensity measurement levels (PGA, Sa) (Silva *et al.* 2013b). Each fragility function was fitted with a cumulative probability curve with a lognormal distribution, whose statistical parameters (i.e., logarithmic mean (ʃ) and logarithmic standard deviation). Fragility functions can be defined as discrete points or continuous (Villar-Vega *et al*. 2017). In seismic risk analysis, the fragility model is used to calculate the damage distribution on a considered region. In addition, fragility models are used to obtain vulnerability curves using specified consequence models.

The probabilistic distribution of the loss ratio across the different seismic intensity levels is defined by the vulnerability functions. Damage-to-loss models with the set of fragility functions developed are used to derive a vulnerability function refers to the ratio of repair to the cost of replacement based on ground motion intensity (Martins *et al.* 2016). Vulnerability curves measure the probable economic loss; the fragility curves measure the probability of damage distribution. Vulnerability curves can be obtained using damage functions and loss models. In the current version of the OpenQuake engine, loss functions defined as discrete are used to directly model losses that may be such as deaths or repair costs (Martins *et al.* 2020). By using the average loss rate corresponding to the seismic intensity level (PGA, PGV, Sa) and the coefficient of variation of this ratio, loss curves can be defined as a probabilistic distribution in OpenQuake engine. The exposure model considered in seismic risk analysis consists of detailed information on assets within the relevant region (Silva *et al.* 2014).

The classical PSHA-based workflow was used to develop a classical probabilistic seismic hazard analysis, taking into account the source models and ground motion prediction equation proposed in the ESHM13 model. The seismic hazard results, physical vulnerability functions, and exposure models were used to perform a Classical PSHA-based risk analysis for a series of return periods (Burton and Silva 2016).

In this study, a probabilistic seismic hazard analysis was performed for the Bandırma-I NGCCP control building, taking into account the tectonic structure, seismicity, and seismic source zoning of the study area with OpenQuake, an open-source program. A probabilistic seismic risk assessment was performed in the assessment of financial loss of the structure, using the results of earthquake hazard analysis.

The field-specific earthquake ground motion spectrum based on probabilistic earthquake hazard calculations performed within the scope of the study was compared with the standard earthquake ground motion spectrum Turkish Seismic Code-2007 (TSC 2007) and Turkey Building Seismic Design Code-2018 (TBSDC 2018). Because it is concluded as to use the well-correlated spectra in scaling in determining the spectrum compatible acceleration data set based on comparison of spectra. 5% damping spectrum curves obtained by considering soil effects and near-fault effects and TBSDC 2018 horizontal response spectrums are constructed for 43, 72, to 475, and 2475 years recurrence periods.

Earthquake level according to TBSDC 2018 is classified as :

• DD-1=Earthquake ground motion level with 2% probability of exceedance in 50 years (recurrence period 2475 years)

• DD-2=Earthquake ground motion level with 10%

probability of exceedance in 50 years (recurrence period 475 years)

• DD-3=Earthquake ground motion level with 50% probability of exceedance in 50 years (recurrence period 72 years)

• DD-4=Earthquake ground motion level with 68% probability of exceedance in 50 years (recurrence period 43 years).

Fig. 5 shows the TBSDC 2018 design spectrum. Spectrum details are explained in TBSDC 2018, Chapter 2.

3. Calculation

3.1 Marmara region earthquake hazard analysis

In OpenQuake engine, seismic risk analysis flowchart is existed for scenario-based risk analysis, classical probabilistic risk analysis and (or) event based probabilistic risk analysis. Seismic risk analysis is performed using the results obtained from seismic hazard analysis. In this study, probabilistic earthquake hazard analysis calculations were performed for the Marmara region and the location of the Bandırma-I NGCCPP control building using the OpenQuake seismic hazard and risk program. The seismic area source, line source, and background source models defined in the SHARE project (Woessner *et al.* 2015) were used in this study. Akkar and Boomer (2010) , Cauzzi and Faccioli (2008), Chiou and Youngs (2008), Zhao *et al.* (2006) models were used as ground motion prediction equations (GMPE) to process seismic hazard analysis. Seismic hazard analysis has been completed for 50 years. Two different probabilistic seismic hazard analyses, soil dependent, and soil independent, were carried out. The shear wave velocity (V_{s30}) at 30 m depth was defined as 760 m / s for the soil independent case. For the soil-dependent case, the shear wave velocity (V_{s30}) at 30 m depth was defined as 360 m/s. With reference to the NEHRP (FEMA-356, 2000) soil classification, the value of V_{s30} = 760 m/s was considered as ZB soil class, and V_{s30} = 360 m/s as ZD soil class. As a result of probabilistic seismic hazard analysis with OpenQuake, PGA and Sa distributions in the Marmara region were examined for earthquake hazard levels with 2475 and 475 year return periods.

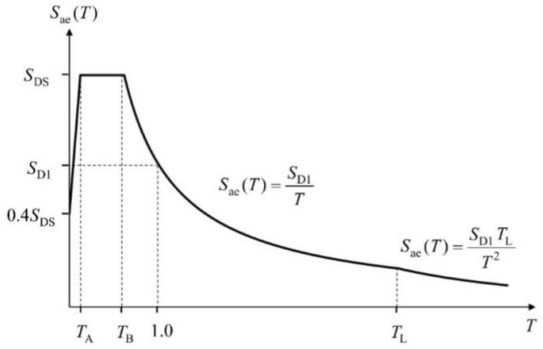

Fig. 5 TBSDC2018-Horizontal elastic design acceleration spectrum with 5% damping (TBSDC 2018)

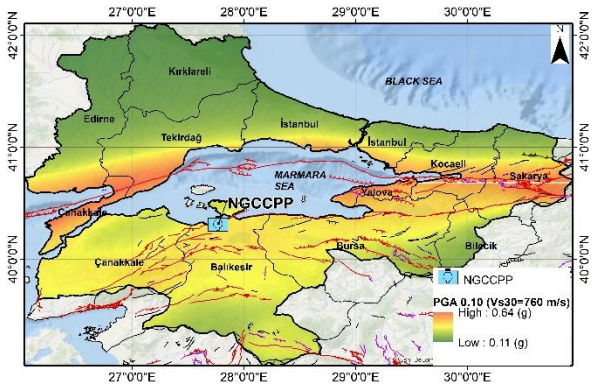

Fig. 6 PGA Distribution in Marmara Region for V_{s30} = 760 m / s, 475 years

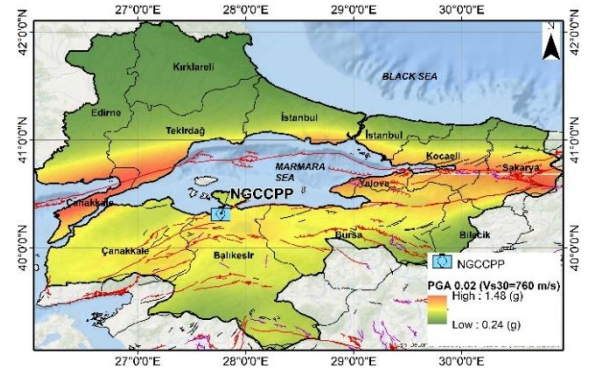

Fig. 7 PGA Distribution in Marmara Region for V_{s30} = 760 m/s, 2475 years

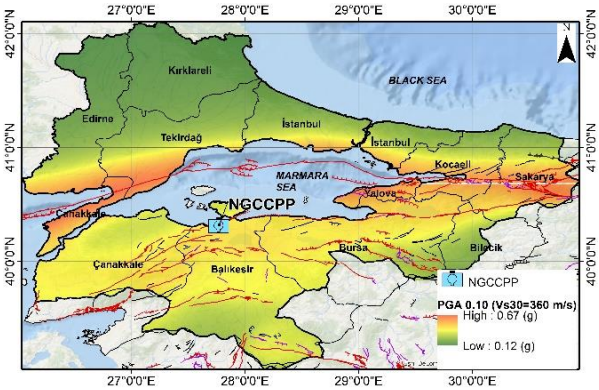

Fig. 8 PGA Distribution in Marmara Region for V_{s30} = 360 m/s, 475 years

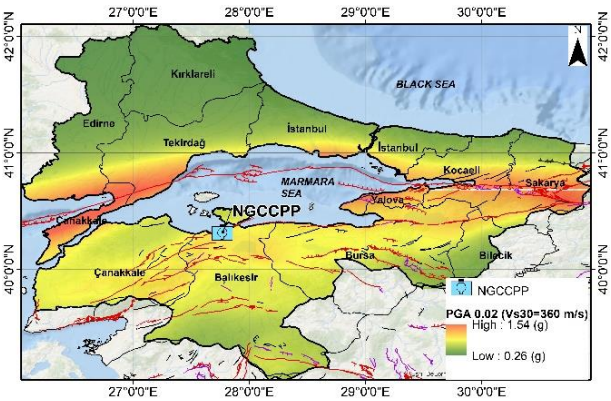

Fig. 9 PGA Distribution in Marmara Region for V_{s30} = 360 m/s, 475 years

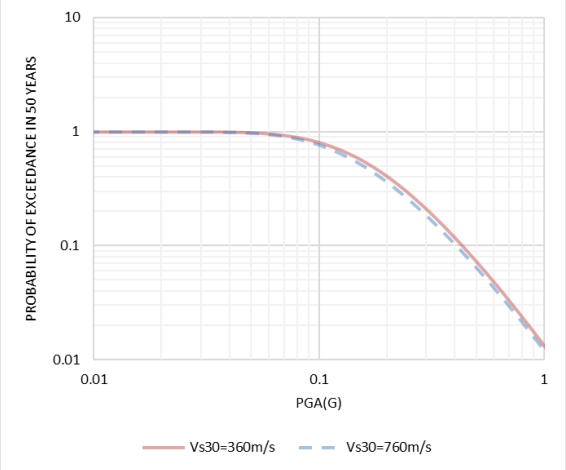

Fig. 10 Hazard curves of Bandırma-I NG CCPP, control building for soil dependent and soil independent cases

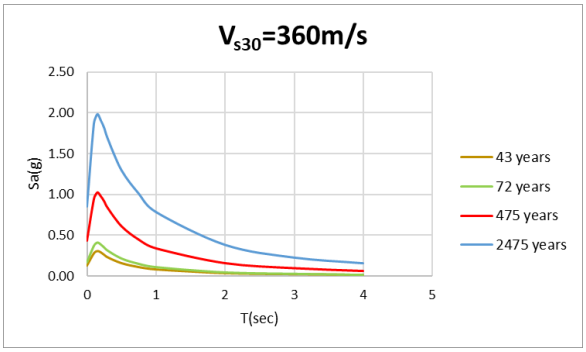

Fig. 11 5% Damped Spectrum Curve of Bandırma-I NG CCPP, control building for soil dependent cases for each earthquake return period)

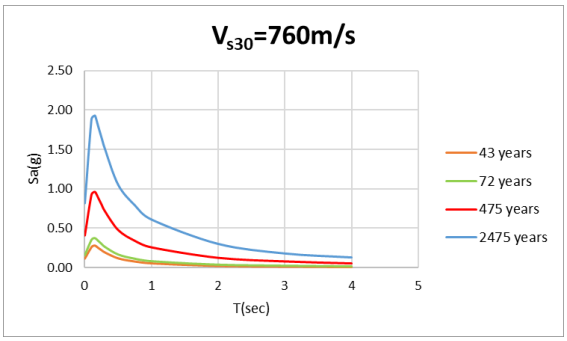

Fig. 12 5% Damped Spectrum Curve of Bandırma-I NG CCPP, control building for soil independent cases for each earthquake return period)

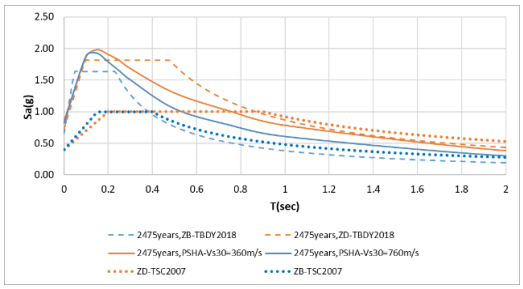

Fig. 13 Comparison of hazard spectra with TBSDC 2018 spectra for earthquakes with a return period of 2475 years (DD-2) for ZB (V_{s30} = 760 m/s) and ZD (V_{s30} = 360 m/s) soil conditions

As a result of the probabilistic seismic hazard analysis, the PGA distribution for the earthquake hazard level with a return period of 475 and 2475 years for the soil independent condition is given in Figs. 6 and 7, respectively.

Similarly, as a result of the probabilistic seismic hazard analysis, the PGA distribution for the earthquake hazard level with 475 and 2475 year return periods for the soil-dependent situation is given in Figs. 8 and 9, respectively.

It has been determined that the soil condition of the location of Bandırma-I NGCCPP is weak. It has been determined as V_{s30} = 360 m/s in the soil studies of the region. For the soil-dependent situation, the shear wave velocity at 30 m depth (V_{s30}) was defined as 360 m/s for hazard analysis. According to NEHRP-FEMA-356 (2000) soil classification, V_{s30} value indicates that it is ZD soil class. As shown in Fig. 10, hazard curves were obtained logarithmically for the soil dependent (V_{s30} = 360 m/s) and soil independent (V_{s30} = 760 m/s) cases belonging to Bandırma I.

As a result of the probabilistic earthquake hazard analysis, 5% damped spectrum curves for soil dependent and soil independent conditions for the Bandırma-I NGCCP control building were obtained for each earthquake recurrence period (43 years, 72 years, 475 years, 2475 years). In Figs. 11 and 12, spectrum curves obtained for two different soil conditions according to each earthquake recurrence period for the Bandırma-I NGCCP control building are shown.

The spectrum curves obtained are comparatively analyzed considering the spectra presented in TBSDC 2018 for 5% damped DD-1, DD-2 earthquake hazard levels, and the design spectra presented in TSC 2007 for the first-degree earthquake zone. This comparison was shown in Figs.13 and 14, respectively. In this comparison, the spectra for the soil-dependent case (ZD soil class) and for the soil independent case (ZB soil class) presented in the regulations were considered.

As clearly seen in Fig. 13, TBSDC 2018 spectrum and TSC 2007 spectrum for ZD (V_{s30} = 360 m/s), ZB (V_{s30} = 760 m/s) soil condition, DD-1 earthquake level are more it remains at a lower level. Therefore, spectra obtained as a result of probabilistic hazard analysis for earthquake level DD-1, ZD, and ZB ground conditions are valid for scaling the acceleration records that should be used in seismic design.

As shown in Fig. 14, the spectrum obtained from site-specific seismic hazard analysis for ZD (V_{s30} = 360 m/s), ZB (V_{s30} = 760 m/s) soil conditions, were compared to TBSDC 2018 spectrum for DD-2 earthquake level and first-degree earthquake zone the TSC 2007 design spectrum. In the short period of ZB ground conditions, the field-specific spectrum remains higher than the TBSDC 2018 and TSC 2007 spectrum, while the TBSDC 2018 spectrum remains at a higher level in ZD ground conditions. Therefore, the spectrum obtained as a result of probabilistic hazard analysis for the ZB soil condition at the earthquake level

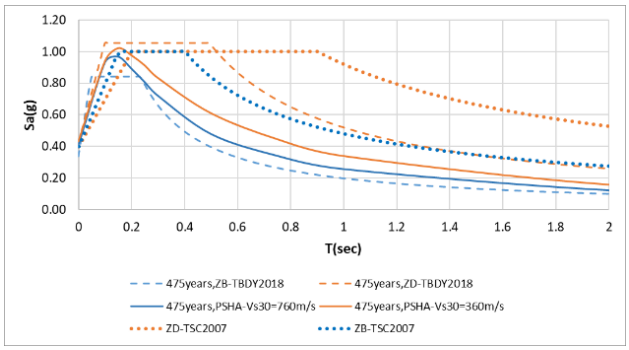

Fig. 14 Comparison of hazard spectra with TBSDC 2018 spectra for earthquakes with a return period of 475 years (DD-2) for ZB (V_{s30} = 760 m/s) and ZD (V_{s30} = 360 m/s) soil conditions)

Fig. 15 EnerjiSA Üretim Bandırma-I NG CCPP, Control Building General View

DD-2 in the low period range is valid for scaling the acceleration records that should be used in seismic design. For the entire period range, it is necessary to use the TBSDC 2018 design spectrum for scaling the acceleration record in the region for ZD soil conditions.

The seismic hazard curve obtained from the probabilistic seismic hazard analysis will be taken into account in the economic loss estimation based on the probabilistic seismic risk assessment for the Bandırma-I NGCCP control building.

3.2 Bandırma-I NGCCPP, Control Building Earthquake Risk Assessment Analysis

One of the most critical structures in a Power Plant to ensure the continuity of production after natural disasters is the Power Plant Control Building. The entire production process of the power plant is monitored and managed from the Control Room in this building.

The current Control Building, considered within the scope of the study, was designed as a two-story reinforced concrete carcass building with dimensions of 42.1mx 22.6 m. The building carrier system is arranged to consist of reinforced concrete frames and shear walls (Fig. 15).

In addition to the control room, the Control Buildings, the C&I room, battery room, low/medium-voltage rooms, etc., which are very important for the continuity of production in the Power Plant include critical equipment rooms (Figs. 16). This building is the main control center of

Fig. 16 EnerjiSA Üretim Bandırma-I NG CCPP, Control Building Low Voltage Room

the power plant, all signal, and energy cables going to the site are collected in this building.

In this study, a Seismic Risk Analysis was performed for the Control Building, which is critical for the Power Plant. The seismic risk of a certain structure located in a seismic zone is determined by the seismic hazard and its structural vulnerability (Preciado *et al.* 2015). For this, probabilistic seismic hazard analysis results, which are evaluated specifically for the region where the power plant is located, are used. Seismic fragility curves are used to reduce structural losses due to earthquakes and manage risk through seismic risk assessment (Lee and Moon 2014). In the assessment of economic losses, fragility curves and vulnerability curves of the building was defined.

Different analysis methods have been developed for seismic vulnerability and risk assessment of seismically vulnerable regions (Liu *et al.* 2020). The relationship between the intensity of earthquake ground motion and the probability of exceeding certain damage levels is described by seismic fragility curves (Lee *et al.* 2021). Fragility and vulnerability functions usually derived for building type structures in a region do not include other types of structures (Dabbeek *et al.* 2020). Due to the lack of country-specific studies, vulnerability or fragility functions are often used from different regions (Dabbeek *et al.* 2020). For example, Hancilar *et al.* (2018) employed HAZUS-MH MR5 (2014) based functions, to assess seismic risk for Muscat, Oman (Dabbeek *et al.* 2020). The fragility functions considered in this study are derived from HAZUS-MH MR5 (2014) database.

The fragility function is presented in HAZUS-MH MR5 (2014) for slight, medium, extensive, and collapse damage cases of reinforced concrete ductile low-rise reinforced concrete structures was used in the assessment of damage distributions to occur in the structure for any earthquake hazard considered in this study. This curve is presented as a function of maximum ground acceleration (PGA). The fragility curve defined in HAZUS-MH MR5 (2014) for low-rise, ductile, reinforced concrete structures is shown in Fig. 17. For the equipment, the fragility curve defined in HAZUS-MH MR5 (2014) was used as shown in Fig. 18. While the PGA earthquake parameter is considered in the structural damage distribution, the Sa (spectral acceleration) earthquake parameter is taken into consideration in the damage distribution in the equipment.

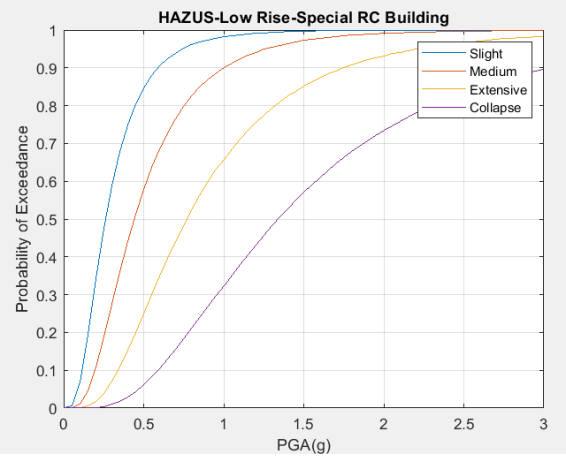

Fig. 17 Fragility curves considered for low-rise reinforced concrete building (HAZUS-MH MR5(2014))

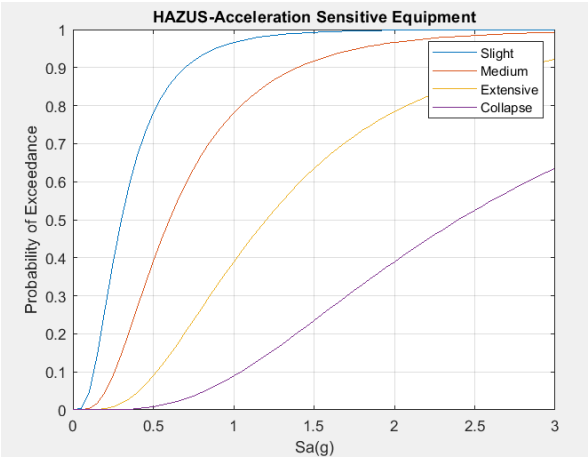

Fig. 18 Fragility curves considered for acceleration sensitive equipment (HAZUS-MH MR5,(2014))

Developing a fragility model is often one of the first steps of a loss estimation study, and this can be combined with an outcome model for a range of loss models and used to assess seismic risk. In this study, fragility models belonging to structural and equipment were transformed into loss models by using the consequence model proposed by HAZUS-MH MR5 (2014). Table 1 defines the average loss ratio for each damage state suggested in the HAZUS-MH MR5 (2014) study. Loss ratio is defined as the ratio of the earthquake damage repairing cost to the replacement cost for the structure (Khanbabazadeh *et al.* 2020). Vulnerability functions can also be created using other fragility functions and consequence functions.

The loss curve used in seismic risk assessment was calculated with Eq. (1) by using the fragility curves together with the consequence models (Martins *et al.* 2016). In Eq. (1), I is the earthquake intensity parameter (PGA, Sa, etc.), i is the value of the earthquake intensity parameter taken into consideration, ds is each damage state (light, medium, heavy, collapse), LR_{ds} shows the average loss ratio (loss ratio) obtained with the consequence models for each damage state. E[LossRatio|I=i]; it shows the expected loss ratio for defined each i which is the earthquake intensity parameter.

Table 1 HAZUS-MH MR5 (2014) Consequence model to drive vulnerability curve

Damage State	Loss ratio
Slight	0.02
Moderate	0.10
Extensive	0.50
Collapse	1.00

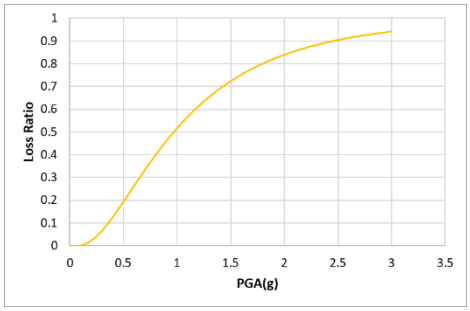

Fig. 19 Vulnerability curve derived from the structural fragility curve

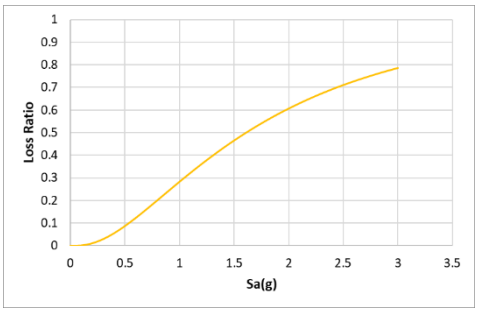

Fig. 20 Vulnerability curve derived from the equipment fragility curve

$$E[LossRatio|I=i] = \sum_{hd=0}^{nHD} (P[DS=ds|I=i].LR_{ds}) \quad (1)$$

By using Eq. (1), the vulnerability curve of the related structure is obtained depending on the considered earthquake intensity parameter. The vulnerability of structural elements and equipments have been obtained as shown in Figs. 19 and 20 by using the consequence model of HAZUS-MH MR5 (2014) and the fragility functions taken from HAZUS in Eq. (1).

4. Results & discussion

Economic losses are calculated by using the vulnerability curves in the earthquake risk analysis model. The loss ratios for each earthquake parameter (PGA, Sa) defined in the vulnerability curves are used together with the probability of exceedance of these earthquake parameters calculated from the earthquake hazard, and the probability of exceedance of economic losses is calculated for the defined time interval. The probability of exceeding loss in 50 years is shown in Figs. 21 and 22 for the soil-

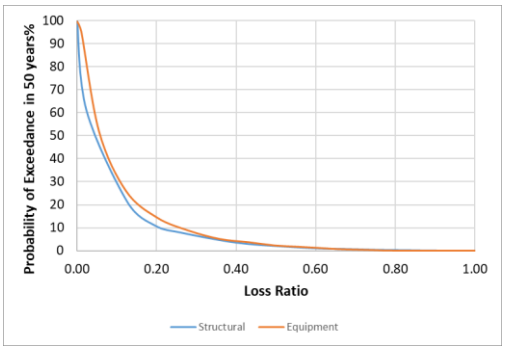

Fig. 21 Probability of exceedance of economical structural and equipment loss ratio curve obtained as a result of risk analysis

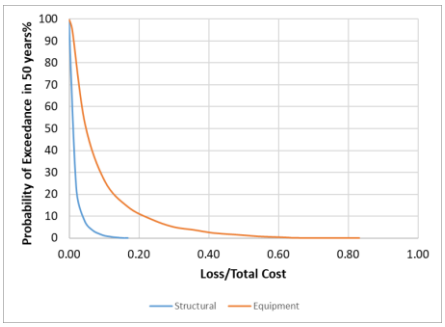

Fig. 22 Probability of exceeding the ratio of the economical structural loss and equipment loss to the total cost obtained as a result of the risk analysis

Table 2 Ratios of economical structural loss and equipment loss to total building cost for different earthquake levels

Earthquake Level	Return Period(year)	Structural Loss/Total Cost	Equipment Loss/Total Cost
DD-1	2475	8.8%	45.7%
DD-2	475	4.0%	23.2%
DD-3	72	1.4%	4.6%
DD-4	43	0.5%	2.5%

dependent case. Table 2 shows the ratio of the amount of structural and equipment financial loss to the total cost for different recurrence earthquake periods. “Total cost” includes building / architectural (structural) and mechanical, electrical, I&C equipment costs (equipment).

As shown in Fig. 21, for earthquakes with exceedance probability above 5% in 50 years, non-structural loss is expected to be greater than structural loss. Since the destructive effects of earthquakes with a probability of exceedance below 5% are expected to be high, structural damage is expected to be large. In such a case, the ratio of structural and non-structural loss is similar.

As a result of the probabilistic earthquake risk analysis, as shown in Fig. 22 and Table 2, the ratio of economic loss to total cost with the probability of exceeding 2% (2475 years) in 50 years, was calculated as 45.7% for equipment and 8.8% for the building. The ratio of the economic loss to the total cost with the probability of exceedance in 50 years is 10% (475 years), was calculated as 23.2% for equipment and 4% for the building. The ratio of the economic loss to the total cost with the probability of exceedance in 50 years is 50% (72 years) was calculated as 4.6% for equipment and 1.4% for the building The ratio of economic loss to total cost with a probability of exceedance in 50 years, 68% (43 years) was calculated as 2.5% for equipment and 0.5% for building.

In the near time, on February 6, 2023, at 04.17 and 13.24 local time in Turkey, two earthquakes with an instrumental magnitude (Mw) of 7.8 and 7.6 with epicenters in Pazarcık (Kahramanmaraş) and Elbistan (Kahramanmaraş) occurred 9 hours apart. It was felt in Southeastern Anatolia, Eastern Anatolia, Mediterranean, and Central Anatolia regions. It caused great destruction, damage, and many casualties in many cities located in the Southeastern Anatolia region. During the investigations carried out in the region where these two earthquakes were active, it was determined that there was no Natural Gas Combined Cycle Power Plant. It is known that the earthquakes in the region correspond to the DD-1 earthquake hazard level (2% probability of exceedance in 50 years) stated in TBDY-2018. In such an earthquake, structural damage at almost collapse level is expected. Therefore, in the event of such an earthquake, it is clearly seen that such facilities cannot continue production.

5. Conclusions

Today, electricity generation plays an important role in maintaining socio-economic life. Electricity networks are one of the critical infrastructures with a high probability of damage due to earthquake hazards. Failures in any of the generation facilities, transmission, and distribution networks of these systems will cause interruptions in energy production. This situation may cause the disruption of commercial and industrial activities in the area where the facilities are located. The central building, where all operational activities during the electricity generation phase are controlled by automation method and the continuity of production is ensured, is the control building.

Within the scope of this study, earthquake hazard analysis and risk assessment for the type control building of the "EnerjiSA Üretim Production Bandırma-I Natural Gas Combined Cycle Power Plant" in which the production capacity and components are explained in detail, were performed by considering the tectonic structure, seismicity and seismic source zoning of the area through OpenQuake. For the seismic risk analysis, probabilistic earthquake hazard analysis results, which are evaluated specifically for the region where the power plant is located, are used. In the assessment of damage and loss, fragility curves of the structure and equipment and the consequence model were used. The site-specific earthquake ground motion spectra obtained from the probabilistic earthquake hazard analysis were compared with the TSC 2007 and TBSDC 2018 standard earthquake ground motion spectra. The spectra obtained as a result of probabilistic hazard analysis for DD-1 earthquake level, ZD and ZB ground conditions are valid

for scaling the acceleration records that should be used in seismic design. At the DD-2 earthquake level, the spectrum obtained as a result of the probabilistic seismic hazard analysis for the ZB ground condition is valid for scaling the acceleration records that should be used in seismic design, while the TBSDC 2018 design spectrum should be used in scaling the acceleration record in the region for ZD ground conditions.

The loss of the non-structural and structural elements has been calculated similarly as 50% for the DD-1 seismic hazard level. However, the structural loss is obtained as %20 for the DD-2 seismic hazard level, while this value is found as %30 for the non-structural loss. Also, the losses are proportioned to the total cost of the building. As a result of the probabilistic seismic risk analysis, the economic loss as the ratio to the total cost for DD-1 seismic hazard level (the probability of exceedance 2% in 50 years) was calculated as 45.7% for equipment and 8.8% for the structural. For the DD-2 seismic hazard level (the probability of exceedance in 50 years is 10%) the ratio to the total cost was calculated as 23.2% for equipment and 4% for the structural. Regarding the economic loss for nonstructural elements, approximately 50% loss is expected for the DD-1 seismic hazard level. All the above indicate that the economic losses due to equipment damage will be more than the structural damage. In this study, the rapid seismic risk assessment approach for critical energy facilities is explained using fragility and vulnerability curves. It is believed that this study will be beneficial in decision mechanism for business continuity planning of existing critical facilities. As part of the seismic risk assessment, the study is also important for leading further assessment of business losses and determination of insurance costs.

References

Akkar, S. and Bommer, J.J. (2010), "Empirical equations for the prediction of PGA, PGV, and spectral accelerations in Europe, the Mediterranean region, and the Middle East", *Seismol. Res. Lett*., **81**(2), 195-206. https://doi.org/10.1785/gssrl.81.2.195.

Buriticá Cortés, J.A., Sánchez-Silva, M. and Tesfamariam, S. (2015), "A hierarchy-based approach to seismic vulnerability assessment of bulk power systems", *Struct. Infrastruct. Eng*., **11**(10), 1352-1368. https://doi.org/10.1080/15732479.2014.964732.

Burton, C.G. and Silva, V. (2016), "Assessing integrated earthquake risk in OpenQuake with an application to Mainland Portugal", *Earthq. Spectra*, **32**(3), 1383-1403. https://doi.org/10.1193/120814EQS20.

Cauzzi, C. and Faccioli, E. (2008), "Broadband (0.05 to 20 s) prediction of displacement response spectra based on worldwide digital records", *J. Seismology*, **12**(4), 453. https://doi.org/10.1007/s10950-008-9098-y.

Chiou, B.J. and Youngs, R.R. (2008), "An NGA model for the average horizontal component of peak ground motion and response spectra", *Earthq. Spectra*, **24**(1), 173-215. https://doi.org/10.1193/1.2894832.

Cornell, C.A. (1968), "Engineering seismic risk analysis", *Bull. Seismol. Soc. Am.*, **58**(5), 1583-1606. https://doi.org/10.1785/BSSA0580051583.

Dabbeek, J., Silva, V., Galasso, C. and Smith, A. (2020), "Probabilistic earthquake and flood loss assessment in the Middle East", *Int. J. Disaster Risk Reduction*, **49**, 101662. https://doi.org/10.1016/j.ijdrr.2020.101662.

Eidinger, J., Davis, C., Tang, A. and Kempner, L. (2012), "M 9.0 Tohoku earthquake March 11 2011 performance of water and power systems", *G & E Engineering Systems Inc*, Oakland, CA.

FEMA 356 (2000), NEHRP guidelines for the seismic rehabilitation of buildings. Federal Emergency Management Agency, Washington.

FEMA E-74 (2011), NEHRP a practical guide for the Reducing the Risks of Nonstructural Earthquake Damage. Federal Emergency Management Agency, Washington.

FEMA, HAZUS-MH MR5 (2014), Technical Manual, Department of Homeland Security - Federal Emergency Management Agency, Washington, D.C.

Fujino, Y., Siringoringo, D.M. and Abe, M. (2009), "The needs for advanced sensor technologies in risk assessment of civil infrastructures", *Smart Struct. Syst*., **5**(2), 173-191. https://doi.org/10.12989/sss.2009.5.2.173.

Giovinazzi, S., Wilson, T.M., Davis, C., Bristow, D., Gallagher, M., Schofield, A. and Tang, A. (2011), "Lifelines performance and management following the 22 February 2011 Christchurch earthquake", New Zealand: highlights of resilience. https://doi.org/10.5459/bnzsee.44.4.402-417.

Howard, S., Riker, C., Knight, B. and Knoles, S. (2015), "Innovative analysis and seismic retrofit of 500 kV flexible bus substation support structures", *Electrical Transmission and Substation Structures 2015*, 438-451. https://doi.org/10.1061/9780784479414.035.

Kepenek, E., Korkmaz, K.A. and Gencel, Z. (2020), "Seismic risk investigation for reinforced concrete buildings in Antalya, Turkey", *Comput. Concrete*, **26**(3), 203-211. https://doi.org/10.12989/cac.2020.26.3.203.

Khanbabazadeh, H., Zulfikar, A.C. and Yesilyurt, A. (2020), "Basin edge effect on industrial structures damage pattern at clayey basins", *Geomech. Eng.*, **23**(6), 575-585. https://doi.org/10.12989/gae.2020.23.6.575.

Kwasinski, A., Eidinger, J., Tang, A. and Tudo-Bornarel, C. (2014), "Performance of electric power systems in the 2010-2011 christchurch, new zealand, earthquake sequence", *Earthq. Spectra*, **30**, 205-230.

Lee, Y.J. and Moon, D.S. (2014), "A new methodology of the development of seismic fragility curves", *Smart Struct. Syst.*, **14**(5), 847-867. https://doi.org/10.12989/sss.2014.14.5.847.

Lee, S., Moon, D.S., Kim, B., Kim, J. and Lee, Y.J. (2021), "Hybrid fragility curve derivation of buildings based on post-earthquake reconnaissance data", **28**(4), 553-566. https://doi.org/10.12989/sss.2021.28.4.553

Li, W., Zhou, J., Xie, K. and Xiong, X. (2008), "Power system risk assessment using a hybrid method of fuzzy set and Monte Carlo simulation", *IEEE T. Power Syst.*, **23**(2), 336-343. https://doi.org/10.1109/PES.2009.5275942.

Liu, Y., So, E., Li, Z., Su, G., Gross, L., Li, X. and Wu, L. (2020), "Scenario-based seismic vulnerability and hazard analyses to help direct disaster risk reduction in rural Weinan, China", *Int. J. Disaster Risk Reduction*, **48**, 101577. https://doi.org/10.1016/j.ijdrr.2020.101577.

Martins, L. and Silva, V. (2021), "Development of a fragility and vulnerability model for global seismic risk analyses", *Bull. Earthq. Eng.*, **19**(15), 6719-6745. https://doi.org/10.1007/s10518-020-00885-1.

Martins, L., Silva, V., Marques, M., Crowley, H. and Delgado, R. (2016), "Development and assessment of damage-to-loss models for moment-frame reinforced concrete buildings", *Earthq. Eng. Struct. D.*, **45**(5), 797-817. https://doi.org/10.1002/eqe.2687.

Massie, A. and Watson, N.R. (2011), "Impact of the Christchurch earthquakes on the electrical power system infrastructure", *Bull. New Zealand Soc. Earthq. Eng.*, **44**(4), 425-430.

https://doi.org/10.5459/bnzsee.44.4.425-430.

Mousapoor, E., Ghiasi, V. and Madandoust, R. (2020), "Macro modeling of slab-column connections in progressive collapse with post-punching effect", *Structures*, **27**, 837-852. https://doi.org/10.1016/j.istruc.2020.06.025.

Pagani, M., Monelli, D., Weatherill, G., Danciu, L., Crowley, H., Silva, V. and Vigano, D. (2014), "OpenQuake engine: An open hazard (and risk) software for the global earthquake model", *Seismol. Res. Lett.*, **85**(3), 692-702. https://doi.org/10.1785/0220130087.

Park, J., Nojima, N. and Reed, D.A. (2006), "Nisqually earthquake electric utility analysis", *Earthq. Spectra*, **22**(2), 491-509. https://doi.org/10.1193/1.2198872.

Pinho, R. (2012), "GEM: a participatory framework for open, state-of-the-art models and tools for earthquake risk assessment", *Proceedings of the 15th World Conference on Earthquake Engineering*, Lisbon.

Pourkeramat, P., Ghiasi, V. and Mohebi, B. (2021), "The effect of post-earthquake fire on the performance of steel moment frames subjected to different ground motion intensities", *Int. J. Steel Struct.*, **21**, 1197-1209. https://doi.org/10.1007/s13296-021-00496-9.

Preciado, A., Ramirez-Gaytan, A., Salido-Ruiz, R.A., Caro-Becerra, J.L. and Lujan-Godinez, R. (2015), "Earthquake risk assessment methods of unreinforced masonry structures: Hazard and vulnerability", *Earthq. Struct.*, **9**(4), 719-733. https://doi.org/10.12989/eas.2015.9.4.719.

Shinozuka, M., Dong, X., Jin, X. and Cheng, T.C. (2005), "Seismic performance analysis for the ladwp power system", *Proceedings of the 2005 IEEE/PES Transmission & Distribution Conference & Exposition: Asia and Pacific*, IEEE. https://doi.org/10.1109/TDC.2005.1547165.

Silva, V., Crowley, H., Pagani, M., Monelli, D. and Pinho, R. (2014), "Development of the OpenQuake engine, the Global Earthquake Model's open-source software for seismic risk assessment", *Natural Hazards*, **72**(3), 1409-1427. https://doi.org/10.1007/s11069-013-0618-x.

Silva, V., Crowley, H., Varum, H. and Pinho, R. (2015), "Seismic risk assessment for mainland Portugal", *Bull. Earthq. Eng.*, **13**(2), 429-457. https://doi.org/10.1007/s10518-014-9630-0.

TBSDC-2018, Turkish Building Seismic Design Code, Disaster and Emergency Management Authority. Ankara.

Torbol, M. (2015), "Quasi real-time post-earthquake damage assessment of lifeline systems based on available intensity measure maps", *Smart Struct. Syst.*, **16**(5), 873-889. https://doi.org/10.12989/sss.2015.16.5.873.

Transpower (2011a), "4 September 2010 Darfield earthquake. Lessons learned", Transpower New Zealand Limited Internal Report, 30 March 2011.

TSC 2007 (2007), Turkish Seismic Code 2007. Ministry of Public Works and Settlement, Ankara, Turkey.

Hancilar, U., El-Hussain, I., Sesetyan, K., Deif, A., Cakti, E., Al-Rawas, G. and Al-Jabri, K. (2018), "Earthquake risk assessment for the building inventory of Muscat, Sultanate of Oman", *Nat. Hazards*, **93**(3), 1419-1434. https://doi.org/10.1007/s11069-018-3357-1.

Villar-Vega, M., Silva, V., Crowley, H., Yepes, C., Tarque, N., Acevedo, A.B. and María, H.S. (2017), "Development of a fragility model for the residential building stock in South America", *Earthq. Spectra*, **33**(2), 581-604. https://doi.org/10.1193/010716EQS005M.

Woessner, J., Laurentiu, D., Giardini, D., Crowley, H., Cotton, F., Grünthal, G. and Valensise, G. (2015), "The 2013 European Seismic Hazard Model: Key components and results", *Bull. Earthq. Eng.*, **13**, 3553-3596. https://doi.org/10.1007/s10518-015-9795-1.

Yesilyurt, A., Akcan, S.O. and Zulfikar, A.C. (2021), "Rapid power outage estimation for typical electric power systems in Turkey", *Challenge*, **7**(2), 84-92. https://doi.org/10.20528/cjsmec.2021.02.004.

Zhao, J.X., Zhang, J., Asano, A., Ohno, Y., Oouchi, T., Takahashi, T., Ogawa, H., Irikura, K., Thio, H.K., Somerville, P.G., Fukushima, Y. and Fukushima, Y. (2006), "Attenuation relations of strong ground motion in Japan using site classification based on predominant period", *Bull. Seismol. Soc. Am.*, **96**(3), 898-913. https://doi.org/10.1785/0120050122.

GC